

Supplemental Methods

Constructs and transfections

Lentiviral particle expressing human GH1 and control lentiviral particles were generated at the Cedars-Sinai Virus Core facility. hNCC were plated one day before transfections or treatments. Cells were infected with 50 MOI pLV-EF1p-hGH1-IRES-eGFP-WPRE lentiviral particles and 8 µg/mL polybrene added. Control cells were infected with empty pLV-EF1p-mCherry-IRES-eGFP-WPRE lentivector, and cells harvested 7 days after infection, at the time of maximum GFP expression.

Lentiviral particles expressing human TRIM29 shRNAi, GHR shRNAi or non-targeted scramble shRNAi control (GFP Control Lentiviral Particles) (all from Santa Cruz Biotechnology) were received as stock solutions (10^6 IU/200 µM in DMEM). hNCC were infected with 5 MOI of lentiviral particles and 8 µg/mL polybrene was added to the cultures. After overnight culture medium was changed, cells split 48h later, and selected thereafter in 8 µg/mL puromycin and were used after 4th passage.

Protein analysis

Cells were homogenized and lysed in RIPA buffer (Sigma-Aldridge) with protease inhibitors (Sigma-Aldridge). Proteins were separated by SDS-PAGE, electroblotted onto Trans-Blot Turbo Transfer Pack 0.2 µm PVDF membrane (BioRad), and incubated overnight with antibodies, followed by corresponding secondary antibodies (Sigma-Aldridge).

For Western blot analysis, the following primary antibodies were used: TRIM29 recognizes bands at 48-66 kDa range, from Santa Cruz Biotechnologies (#sc-33151,) or Cell Signaling (#5182). Total ATM from Cell Signaling (#2873) or Abcam (ab-82512), phospho-ATM (Ser1981) from Millipore (#05-740) or Cell Signaling (#13050), phospho-H2A.X (Ser139) from Millipore (#05-636) or Cell Signaling (#9718), Rad50, phospho-Rad50 (Ser635), phospho-p53 (Ser15), and MDR1 all from Cell Signaling (#3427, #14223, #9286 and #13978 respectively). STAT5 (# 9363) and phosphoSTAT5 (Tyr694, cat# 4322) were purchased from Cell Signaling also. Tip60 and GAPDH were from Santa Cruz Biotechnologies (#sc-166323 and sc-25778, respectively). DNA-PKcs (#sc-9051) and phospho-DNA-PKcs (Thre2609, #sc-10164) were from Santa Cruz Biotechnologies. Human and rat GH antibodies were obtained from Dr. Albert F. Parlow (National Hormone and Peptide Program, Harbor-UCLA Medical Center, Torrance, CA), or from R&D Systems (#AF-1067). β -actin was purchased from Sigma-Aldridge (#A1978).

For immunohistochemical analysis of human tissue, antibodies to GH were as above or from Lifespan Biosciences (LS-B4199). β -Gal antibodies were from Lifespan Biosciences (LS-B10989). For immunocytochemistry, γ H2A.X (Ser139) from Cell Signaling (#9718) was used, followed by secondary antibodies goat anti-rabbit AlexaFluor 488 or goat anti-mouse Alexa Fluor 568 (Invitrogen). Antigen retrieval was performed in 10 mM sodium citrate, and control reactions were devoid of primary antibodies. Samples were imaged with a Leica TCS/SP spectral confocal scanner (Leica Microsystems, Mannheim, Germany) in dual emission mode to distinguish autofluorescence from specific staining.

Immunoprecipitation and kinase activity

hNCC cells were plated in 10 cm dishes in full PriGrow III media and changed the next day for serum free media (with 0.1% BSA) with 500 ng/mL GH or no GH overnight, then 5 μ M of etoposide was added for 3 h. Cells were trypsinized and counted. 10×10^6 cells were used per immunoprecipitation reaction with 5 μ g/mL of rabbit IgG (RnD Systems) or 5 μ g/mL of total ATM rabbit antibody from Abcam (#ab-82512). Before starting the reaction, 50 μ L aliquots of cell lysates were taken for Western blot to confirm equal protein amount in samples. Immunoprecipitation was performed according to the manual (Immunoprecipitation Kit (Protein A), Roche), with some modifications: after completion of the reaction, agarose beads were washed twice in lysis buffer and then twice in kinase buffer (10 mM Hepes, pH 7.4/10 mM MgCl₂/50 mM NaCl/10 mM MnCl₂) before performing the kinase assay. For the kinase assay, beads were incubated in 50 μ L of kinase buffer containing 50 μ M ATP, p53 peptide (2 μ g of EPPLSQEAFADLWKK, Millipore), and 10 μ Ci of [γ -³²P] ATP (1 Ci = 37 GBq) for 30 min at 30°C. Reactions were terminated with 30% acetic acid (20 μ L), spotted onto P81 paper, washed in 15% acetic acid, air-dried, and counted on a Beckman LS 6000 Scintillation Counter.

Comet assay

The extent of nuclear DNA damage in individual cell was detected by analyzing accumulation of DNA breaks using OxiSelect Comet Assay kit (# STA-350) per manufacturer instruction. Single cells alkaline electrophoresis was used

for 30 min at 1 volt/cm. The level of DNA damage (intensity of the staining) was measured by ImageJ according to the manual as percent of damaged DNA in the tail of the entire cell DNA, and multiplied by the length of the tail (Olive tail moment, tail DNA% x tail moment length). Data were collected from at least 3 independent experiments. In vivo, colon tissue resected from male and female *GHR*^{-/-} and WT mice age 2-7 months, and epithelial mucosal cells gently scraped out, washed in ice-cold PBS, and processed (87). Animal pairs were matched by sex and age. To evaluate DNA damage, at least 1000 nuclei per group were analyzed in colon mucosal cells in vivo, and at least 200 nuclei per group in cultured cells.

Soft agarose assay

hNCC were plated at 25% confluency, media changed the next day for 0.1% BSA (no serum), and 100 ng/mL or 500 ng/mL GH added for 6 h, and then 5 μ M etoposide was added for 24 h or cells were pretreated with GH overnight and etoposide then added for 1 and 3 h (total exposure to GH 24-30 h). Cells were trypsinized and 5000 cells/well plated in soft agarose in PriGrow III media, supplemented with 5% FBS with or without 100 or 500 ng/mL GH in the chamber's upper layer that contains cells. Cells were fed with fresh media with or without GH every 3rd day, and stained on day 13 with MTT and colonies counted. The experiment was conducted in duplicate and repeated twice.

Colony assay

hNCC were plated at concentration 250,000/well in a 6-well plate in PriGrowIII media supplemented with 5% FBS. After 24 h, media was changed for serum-free media supplemented with 0.1% BSA, and 500 ng/mL or no GH was added. After 6 h, 5 μ M etoposide was added for 24 h or for 1 and 3 h. After treatments, drugs were washed out with PBS, cells were trypsinized and plated in media with 5% FBS into 6-well plates at concentrations of 2,000 cells/well. Fresh GH added every third day. The experiment was conducted in duplicate. Colonies were assessed after 8 days.

Cell proliferation assay

hNCC were pretreated with 500 ng/mL or no GH for 6 h and treated with 5 μ M etoposide for 24 h. Cells were then washed, fresh media with 500 ng/mL or no GH was added, and asynchronized cells were pulsed after 72 h with BrdU labeling solution from 5-Bromo-2-deoxy-uridine Labeling and Detection Kit II (Roche) for 1 h at 37°C. Cells were washed, harvested, and fixed in 70% ethanol in 50 mM Glycin solution (pH2.0). Fixed cells were washed with PBS, stained with anti-BrdU antibody followed by chicken-anti-mouse Alexa Fluor 488 secondary antibody (Invitrogen) and analyzed by FACSCanto. Three independent experiments were performed each in triplicate.

Cell cycle assay

hNCC and HCT116 were plated into 6-well plates in triplicate in respective full media. After 24 hours, when cells reached approximately 60% confluency,

media was changed to serum-free media supplemented with 0.1% BSA, and 500 ng/mL hGH was added. Six hours after hGH treatment, 5 μ M etoposide was added; 24 hours later, cells were washed 3 times in PBS, harvested, and fixed in cold 70% ethanol for 1 hour at +4°C, then spun down and again washed in PBS. Cells were stained with propidium iodide (50 μ g/mL) in the presence of 10 μ g/mL RNase A (Active Motif #101249) for 1 hour at room temperature and analyzed by FACS (Fortessa, BD Biosciences, San Jose, CA) with FACS Diva 8.02 software at the Cedars-Sinai Flow Cytometry Core Facility.

Supplemental Figure Legends

SI Figure 1 GH suppresses etoposide-induced DDR. hNCC cells were pretreated with 500 ng/mL GH for 6 h and then treated with etoposide (Etop). Control cells (Cont) were untreated. A-C. ImageJ quantification of protein expression normalized to loading controls. A) Western blot of hNCC harvested 24 h after etoposide treatment. Due to the large differences in scales, RAD50 is depicted separately (right panel). B) Western blot of hNCC harvested 1 and 3 h after etoposide treatment. PhosphoATM is depicted separately (right panel). C) ATM kinase assay. Western blots of total and autophosphorylated ATM in immunoprecipitated samples. In all graphs, results shown are mean \pm SEM of 3-5 independent experiments. Data are graphed as percent of control, but statistical testing performed on raw numbers. Differences were assessed with Tukey-adjusted Mixed Model Regression. * $p < 0.05$; ** $p < 0.01$ vs control; # $p < 0.05$; ## $p < 0.01$ Etop vs Etop + GH. D) Western blot of hNCC harvested at 96 h after etoposide treatment.

SI Figure 2 GH suppresses etoposide-induced DDR in human colon adenocarcinoma HCT116 and in human non-tumorous breast MCF12A cell lines. Cells were pretreated with 500 ng/mL GH for 6 h, treated with 5 μ M etoposide, and harvested 24 h later. A) Western blots. B) ImageJ quantification of protein expression normalized to loading controls. Results shown are mean \pm SEM of 3-5 independent experiments. Due to differences in scales, pp53 in MCF12A is depicted separately. Data are graphed as percent of control, but

statistical testing performed on raw numbers. Differences were assessed with Tukey-adjusted Mixed Model Regression * $p < 0.05$ vs control; # $p < 0.05$; ## $p < 0.01$ Etop vs Etop + GH. C) Comet assay. Results shown are mean \pm SEM of 3 independent experiments for each cell line. Data are graphed as percent of control, but statistical testing performed on raw numbers. Differences were assessed with Tukey-adjusted Mixed Model Regression.

SI Figure 3 GH suppresses phosphorylation of H2AX. A) Representative confocal image of hNCC pretreated with 500 ng/mL GH for 6 h, treated with 5 μ M etoposide, and harvested 24 h later. Green, γ H2AX; blue, DAPI nuclear staining. B) Row data for aggregate measurements of γ H2AX; 20-30 nuclei per image and 5 images per group were analyzed. Control cells were untreated.

SI Figure 4 GH induces TRIM29 and suppresses Tip60 in hNCC cells. hNCC were pretreated with 500 ng/mL GH and treated with 5 μ M etoposide. Western blots of TRIM29 and Tip60 in hNCC harvested 24 h (A) or 1 and 3 h (B) after etoposide treatment. ImageJ quantification of protein expression normalized to loading controls. Results shown are mean \pm SEM of 3-5 independent experiments. Data are graphed as percent of control, but statistical testing performed on raw numbers. Differences were assessed with Tukey-adjusted Mixed Model Regression. * $p < 0.05$ vs control; ## $p < 0.01$ Etop vs Etop + GH treatments.

SI Figure 5 GH induces TRIM29 and suppresses Tip60 in HCT116 cells. HCT116 cells pretreated with 500 ng/mL GH for 6h, treated with 5 μ M etoposide, and harvested 24 h later. A) Representative Western blots from 3 independent experiments are shown. B) ImageJ quantification of protein expression normalized to loading controls. Results shown are mean \pm SEM of 3 independent experiments. Data are graphed as percent of control, but statistical testing performed on raw numbers. Differences were assessed with Tukey-adjusted Mixed Model Regression. * $p < 0.05$ vs control; # $p < 0.05$ Etop vs Etop + GH treatments.

SI Figure 6 GH does not affect MDR1 expression. Western blot of A) hNCC treated with 500 ng/mL GH for 24 h or infected with lentivirus expressing human GH (hGH). B) hNCC pretreated with 500 ng/mL GH for 6 h and treated with 5 μ M etoposide for indicated times. Representative Western blots from 3 independent experiments are shown.

SI Figure 7 GH suppresses DDR in human intestinal organoids. 3-D human intestinal organoids pretreated with 500 ng/mL GH overnight, treated with 5 μ M etoposide for 24 h, and harvested. Western blots of A) TRIM29 and Tip60, and B) DDR. ImageJ quantification of protein expression normalized to loading controls. Results shown are mean \pm SEM of 3 independent experiments. Data are graphed as percent of control, but statistical testing performed on raw numbers. Differences were assessed with Tukey-adjusted Mixed Model

Regression. * $p < 0.05$; ** $p < 0.01$ vs control; # $p < 0.05$; ## $p < 0.01$ Etop vs Etop + GH.

SI Figure 8 GH suppresses DDR in human intestinal organoids. A)

Western blots of 3-D human intestinal organoids pretreated with 500 ng/mL GH overnight, treated with 3 or 5 μ M etoposide for 24 h, and harvested.

Representative blots of 3 independent experiments are shown. B) ImageJ quantification of protein expression normalized to loading controls. Results shown are mean \pm SEM of 3 independent experiments. Data are graphed as percent of control, but statistical testing performed on raw numbers. Differences were assessed with Tukey-adjusted Mixed Model Regression. * $p < 0.05$; ** $p < 0.01$ vs control; # $p < 0.05$; ## $p < 0.01$ Etop vs Etop + GH treatments.

SI Figure 9 GH suppresses endogenous DDR via TRIM/Tip60 pathway

in vitro. Western blots of A) hNCC treated with 500 ng/mL GH for 24 h. ImageJ quantification of protein expression normalized to loading controls. Results shown are mean \pm SEM of 3 independent experiments. * $p < 0.05$; ** $p < 0.01$ vs untreated control. B) hNCC stably expressing sh scramble (Scr) or shTRIM29 RNAi and treated with 500 ng/mL GH for 24 h. ImageJ quantification of protein expression normalized to loading controls. Results shown are mean \pm SEM of 3 independent experiments. Data are graphed as percent of control, but statistical testing performed on raw numbers. Differences were assessed with Tukey-adjusted Mixed Model Regression * $p < 0.05$; ** $p < 0.01$ vs shScr; # $p < 0.05$;

##p<0.01 shScr + GH vs shTRIM29 + GH. C) Western blot of hNCC treated with GH and harvested 24h later.

SI Figure 10 GH suppresses endogenous DDR via TRIM/Tip60

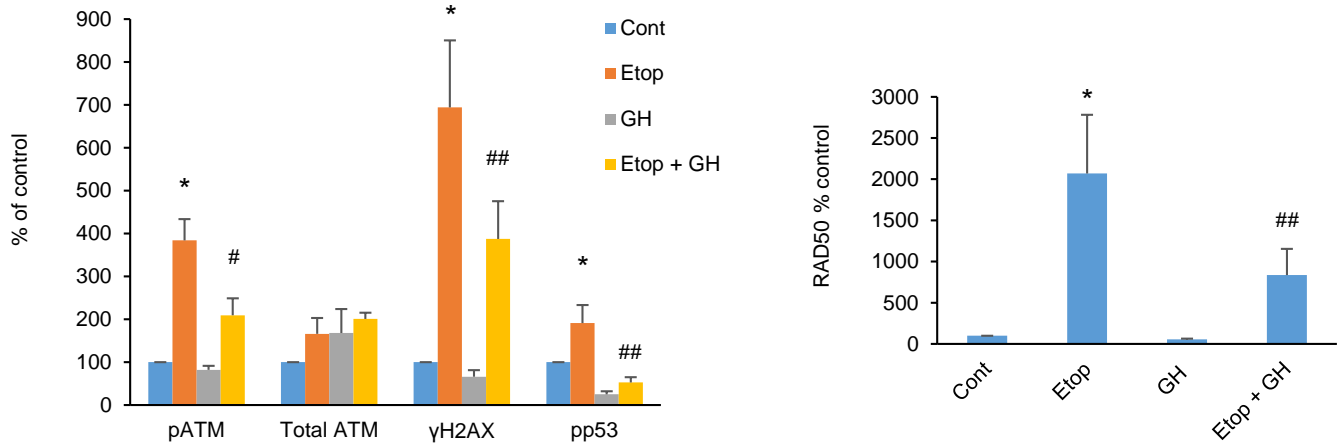
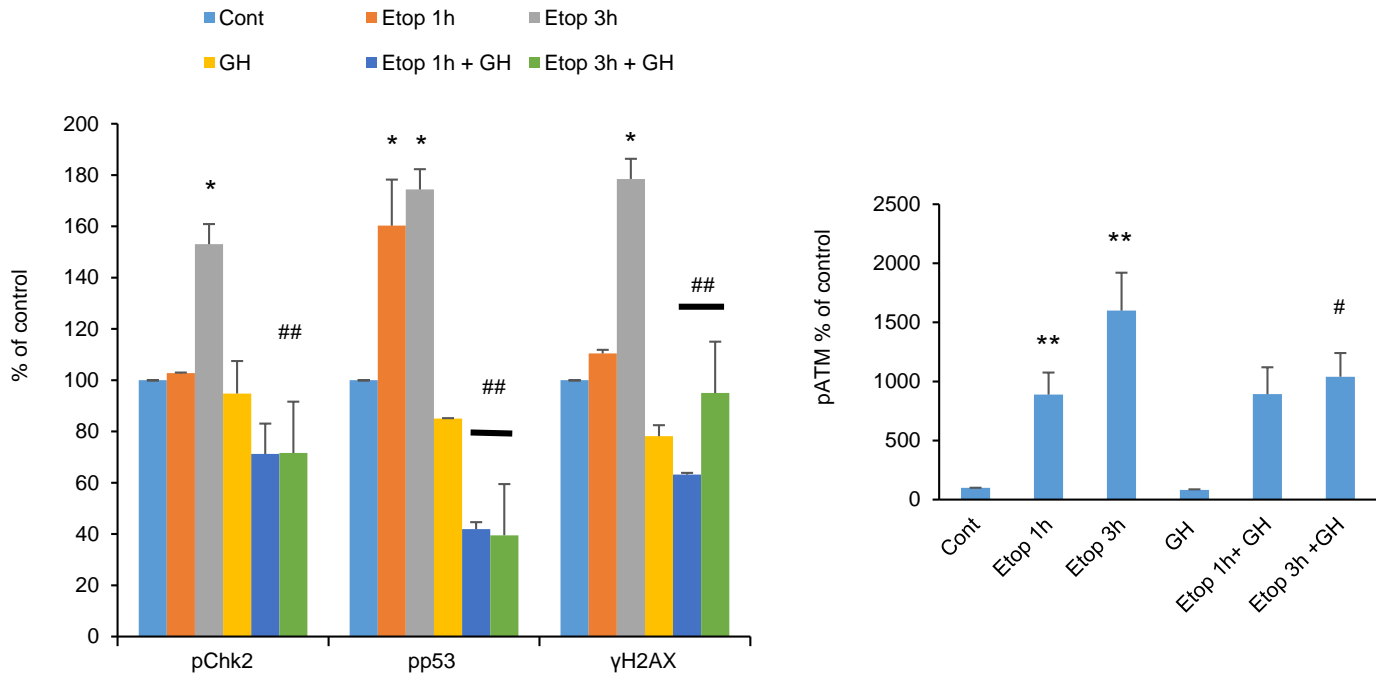
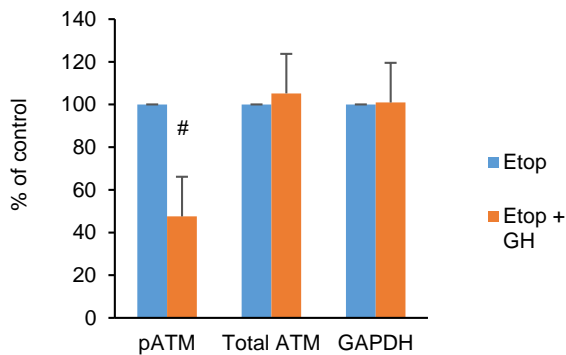
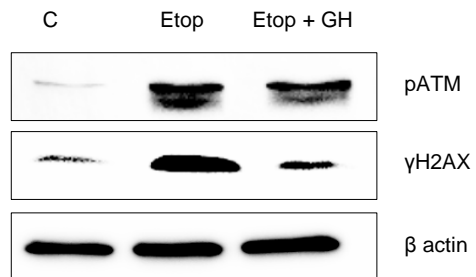
pathway in vivo. Athymic nude mice were injected subcutaneously with 500,000 HCT116 cells stably infected with lenti mGH (GH) or lenti vector. A) Concentration of circulating GH in mice bearing HCT116 lenti mGH or lentiVector xenografts. B) Concentration of circulating GH in mice bearing HCT116 lenti mGH or lentiVector xenografts and intraspleen injected with HCT116 cells. C-D) ImageJ quantification of protein expression normalized to loading controls in C) colon tissue (n=7/group) and D) liver tissues (Vector n=4, GH n=5) derived from mice bearing xenograft tumors. Results were analyzed with two-tailed t-test, **p<0.01 vs control (Vector).

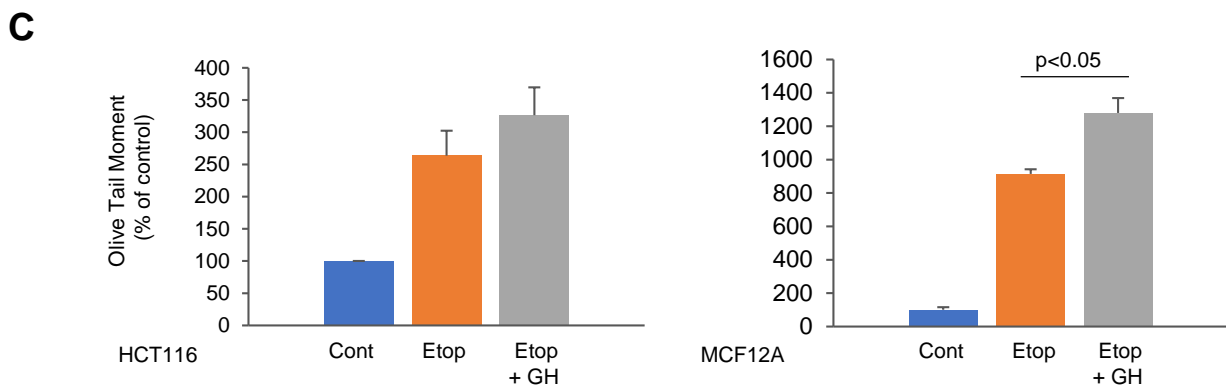
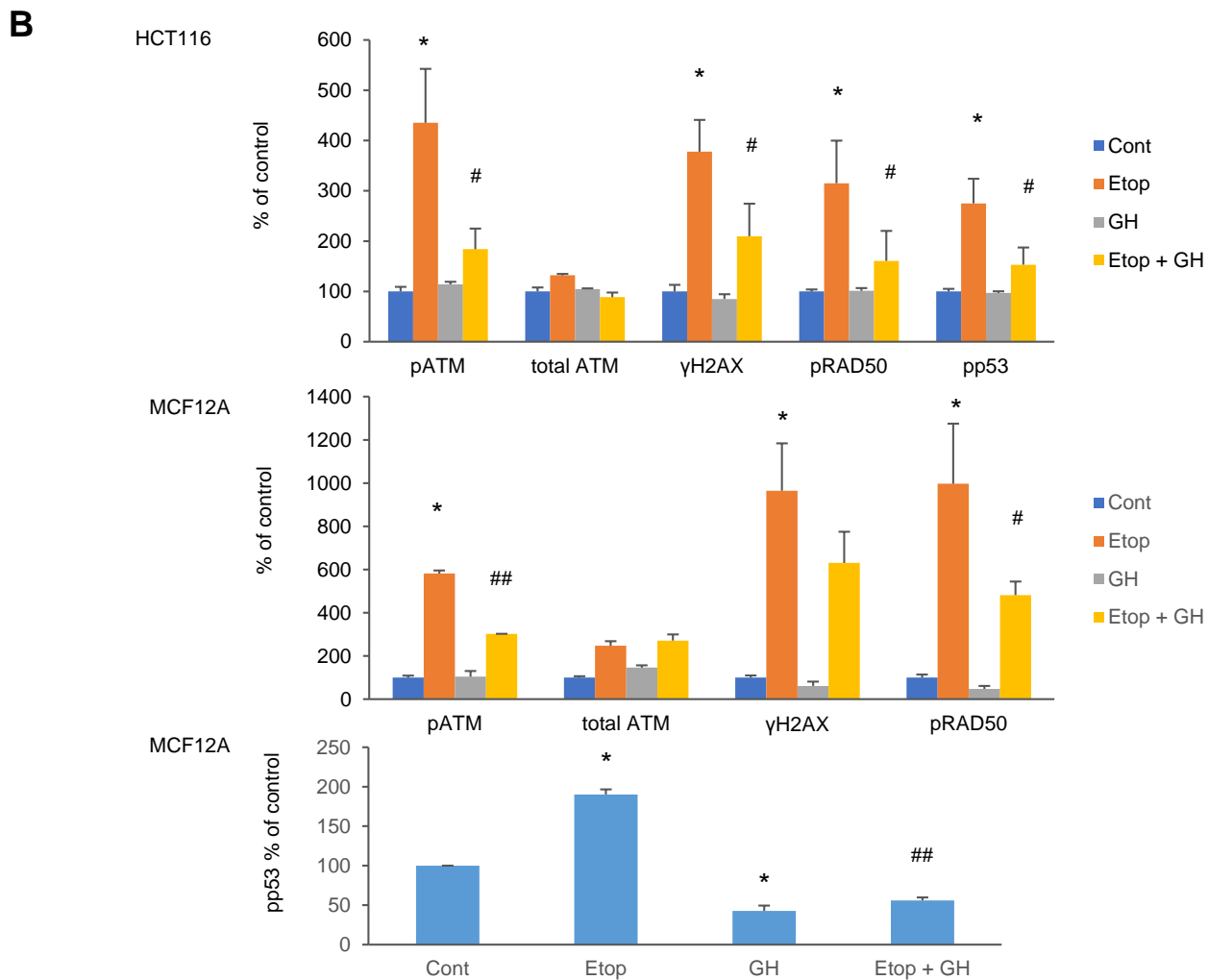
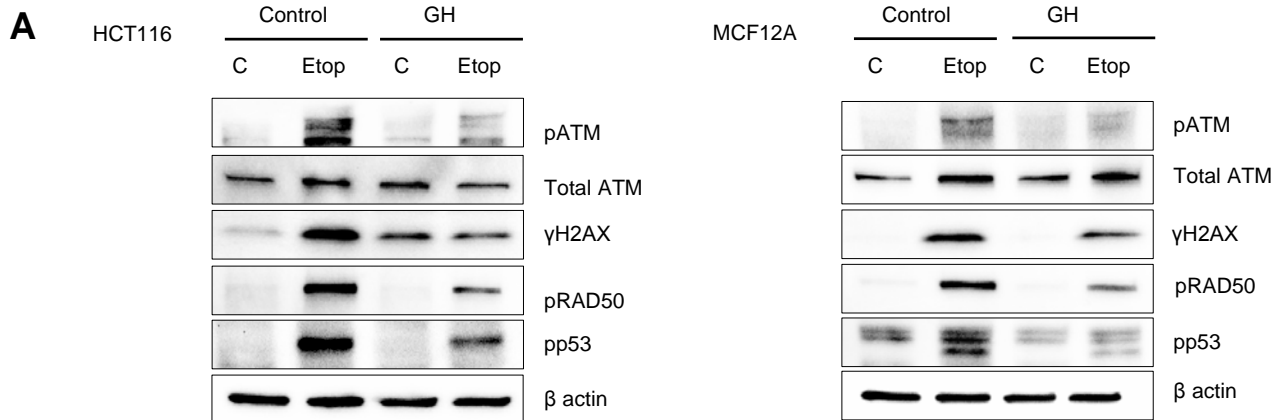
SI Figure 11 GH suppresses DDR via GHR.

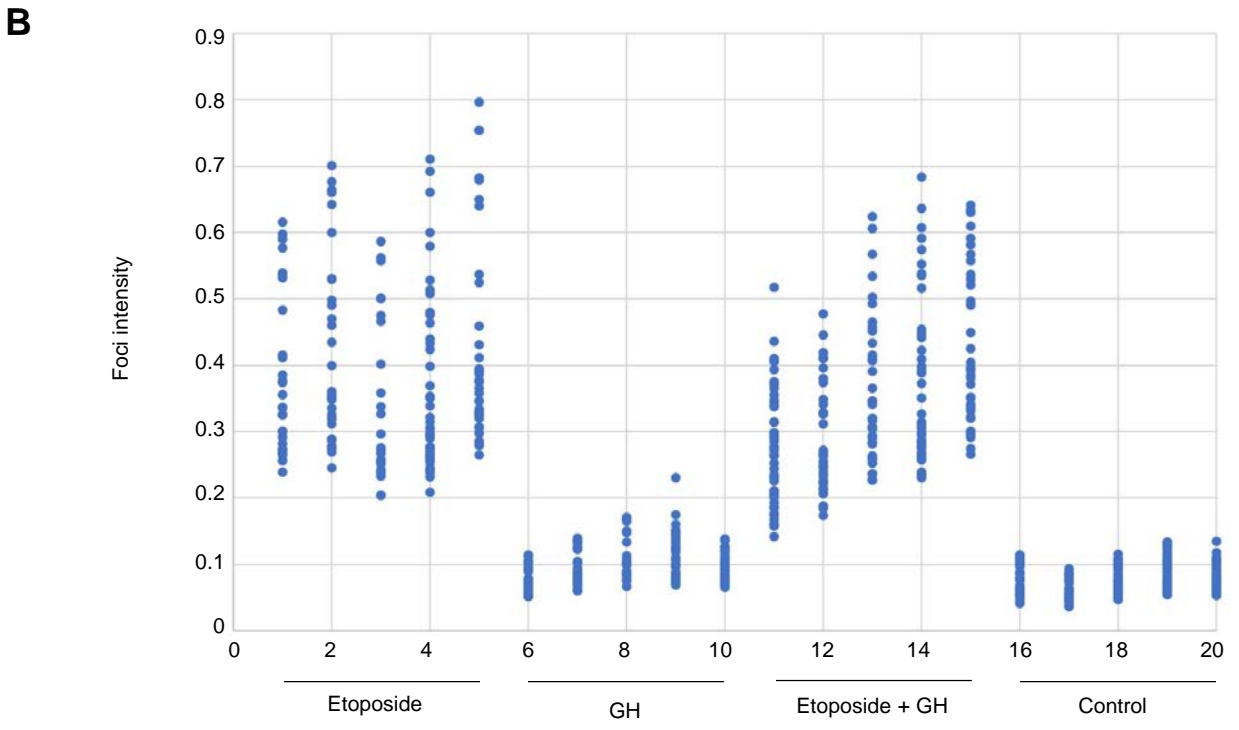
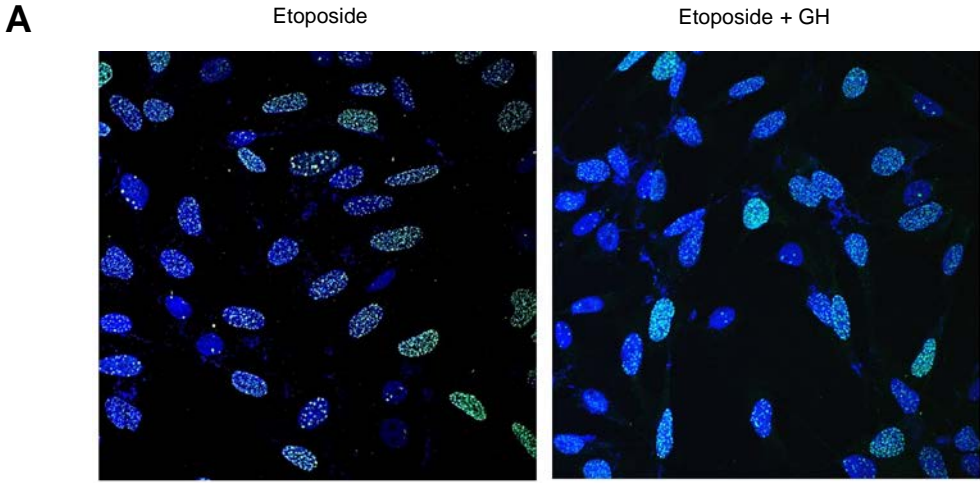
A) hNCC were treated with 20 mg/mL pegvisomant (P) for 1 h and then with 500 ng/mL GH for 24 h. Control cells were untreated. ImageJ quantification of protein expression normalized to loading controls. *p<0.05; **p<0.01 vs control; #p<0.05; ##p<0.01 GH vs P + GH or P. B) GHR and C) phosphoATM expression in hNCC stably expressing shGHR or scramble (Scr) shRNAi and treated with 5 μ M etoposide for 24 h. ImageJ quantification of protein expression normalized to loading controls. *p<0.05; **p<0.01 vs control (shScr); #p<0.05; shScr + Etop vs shGHR + Etop. Results shown are mean \pm SEM of 3 independent experiments. In A-C, data are

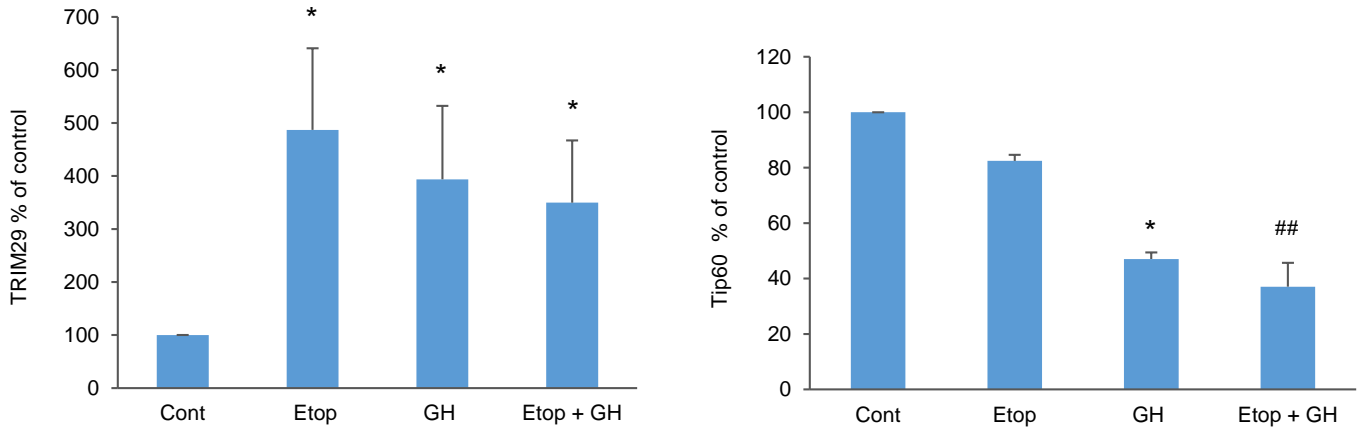
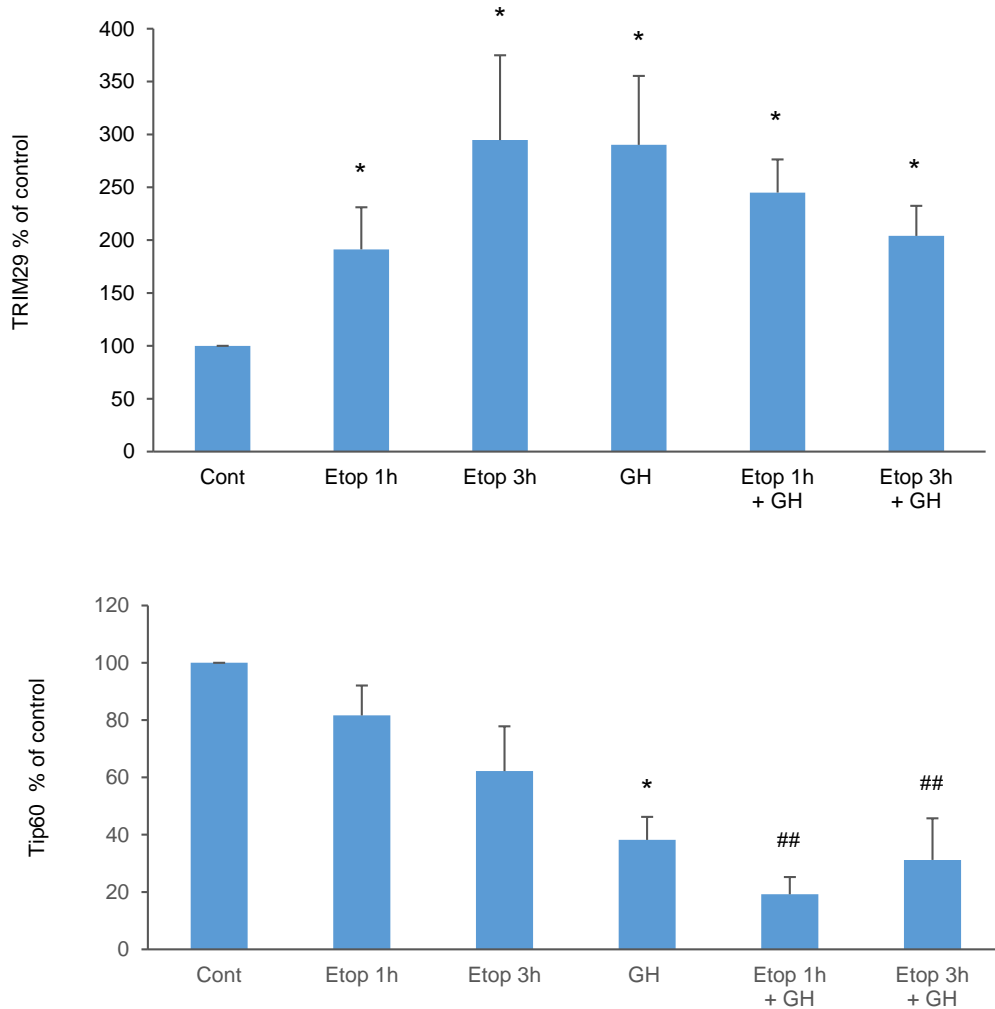
graphed as percent of control, but statistical testing performed on raw numbers. Differences were assessed with Tukey-adjusted Mixed Model Regression.

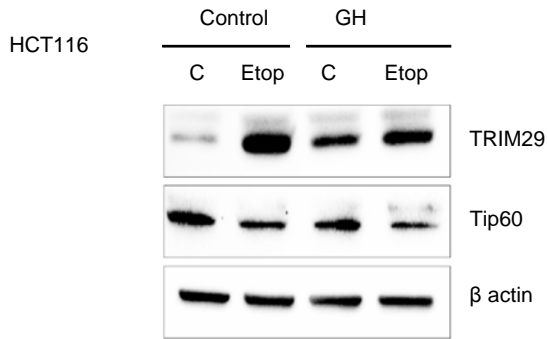
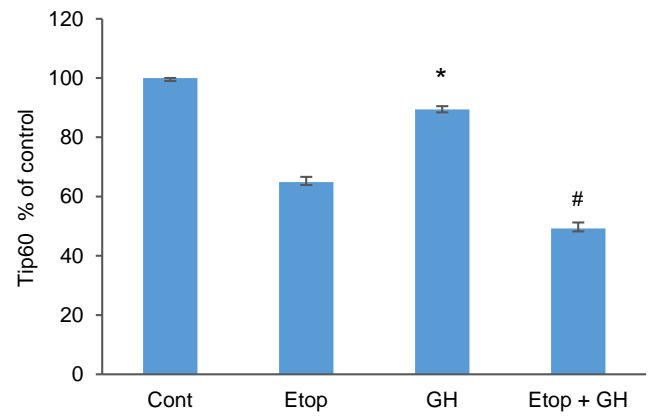
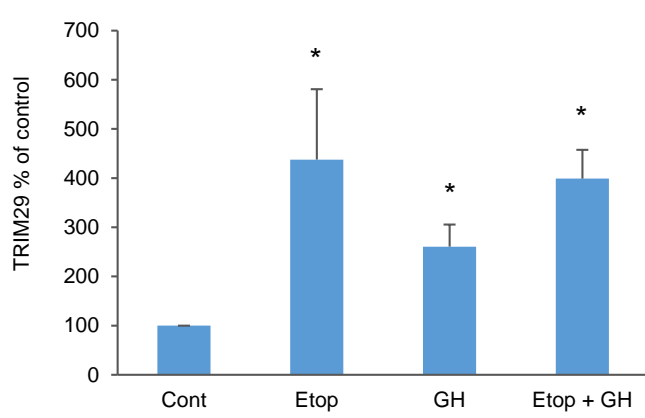
SI Figure 12 GH attenuates endogenous NHEJ DNA repair by inhibiting DNA-PKcs phosphorylation. Western blot analysis of DNA-PKcs phosphorylation in hNCC treated with 500 ng/mL GH for 24 h. ImageJ quantification of protein expression normalized to loading controls. Results shown are mean \pm SEM of 5 independent experiments. $**p < 0.01$ vs control. Data are graphed as percent of control, but statistical testing performed on raw numbers. Differences were assessed with Tukey-adjusted Mixed Model Regression.

A**B****C****D**

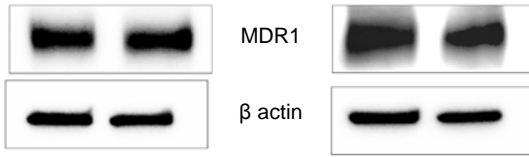




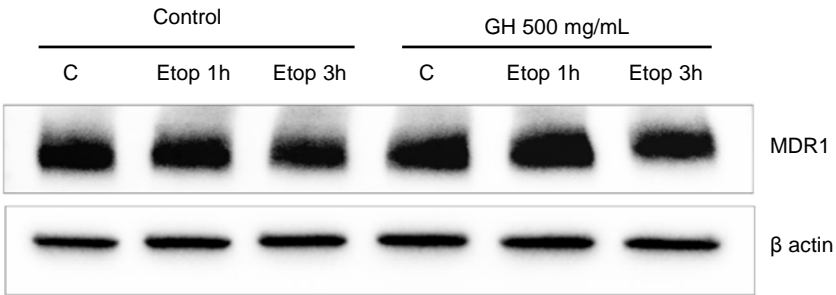
A**B**

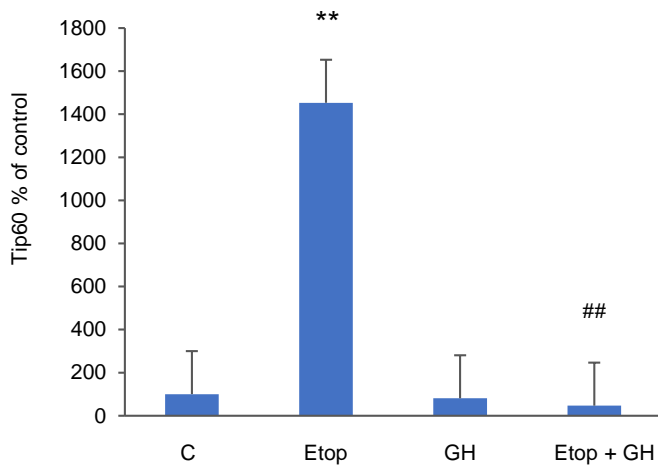
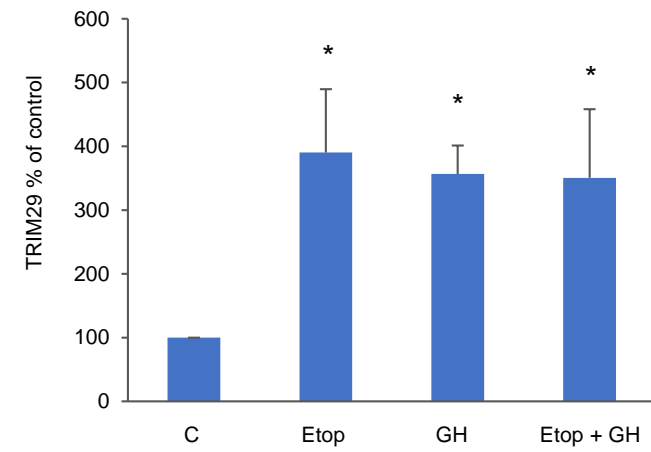
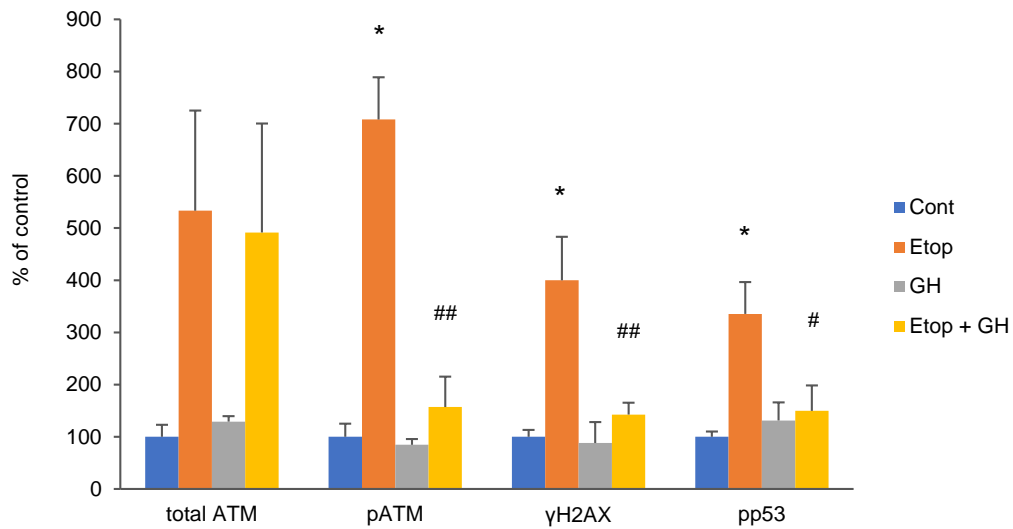
A**B**

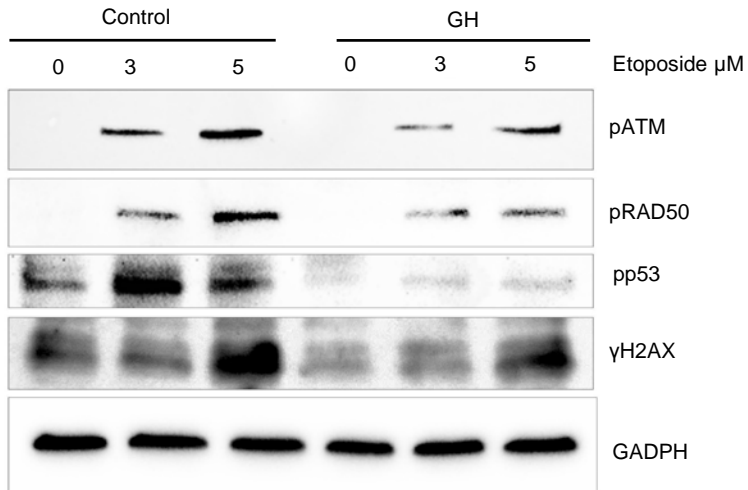
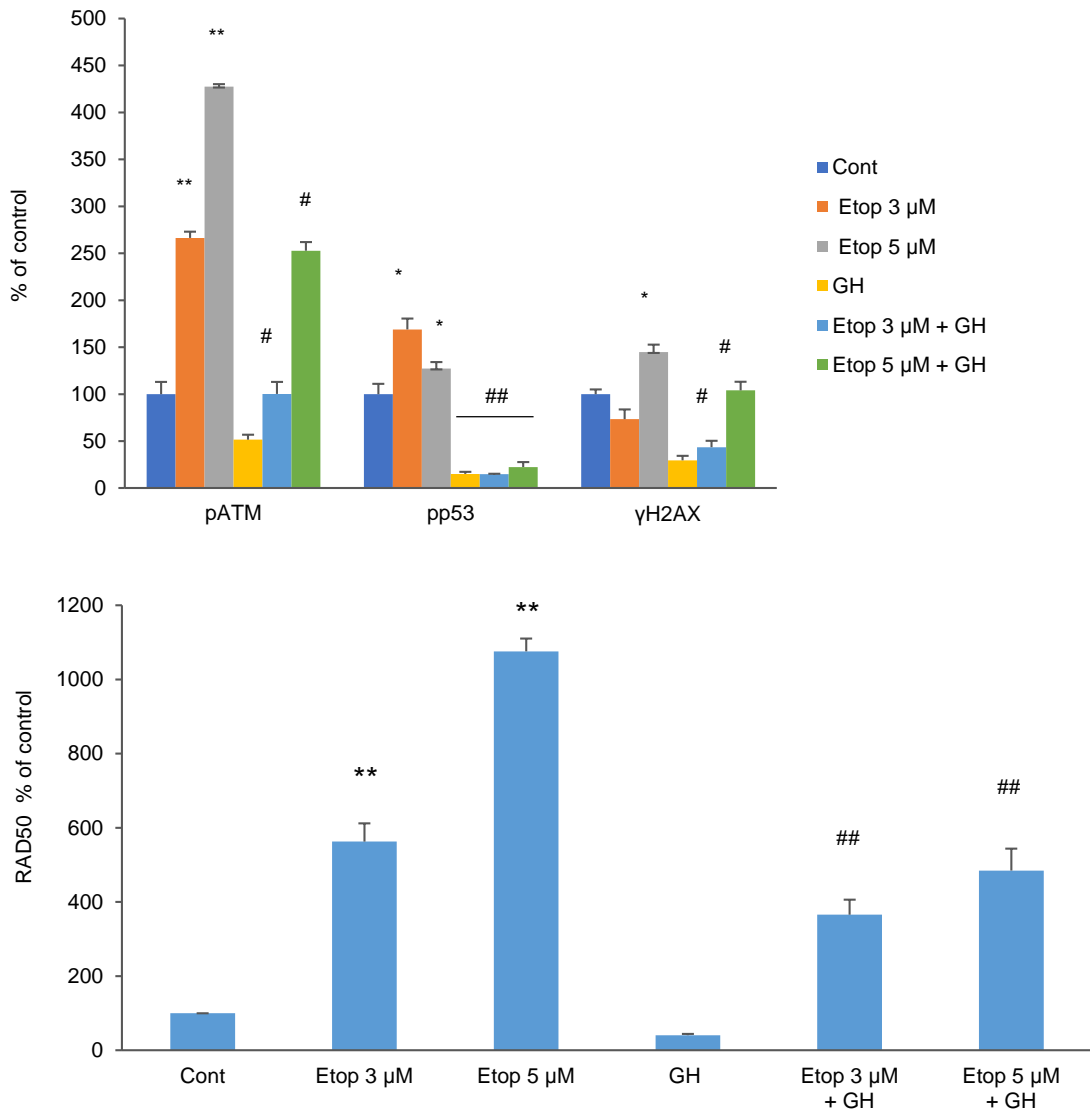
A

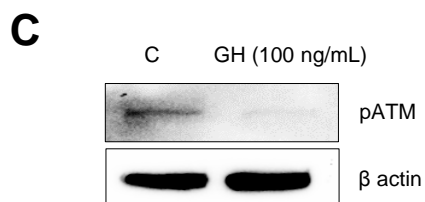
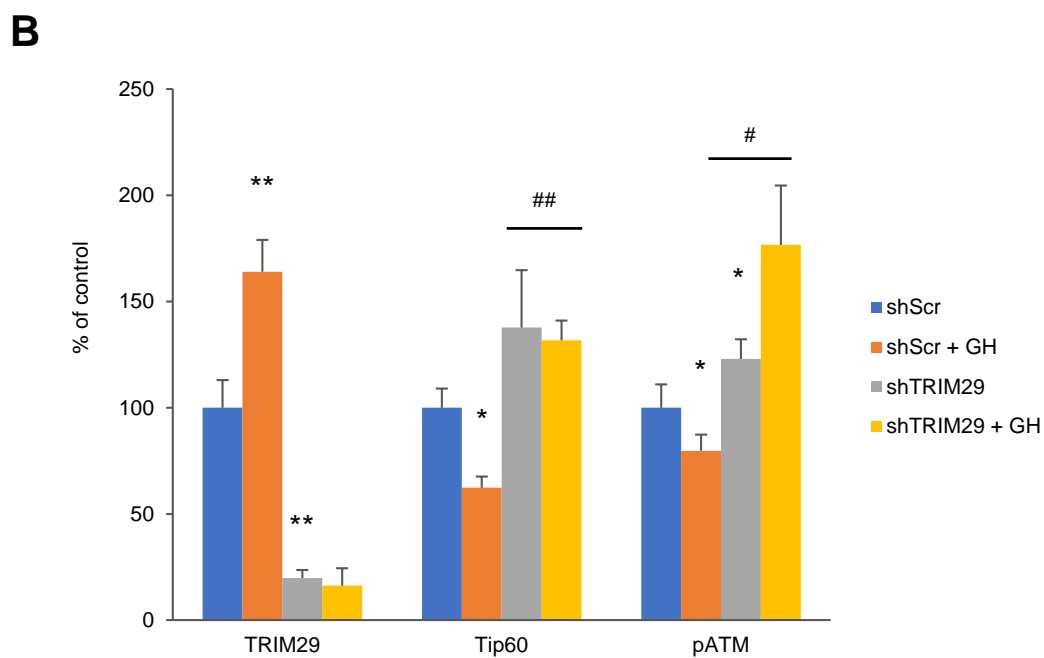
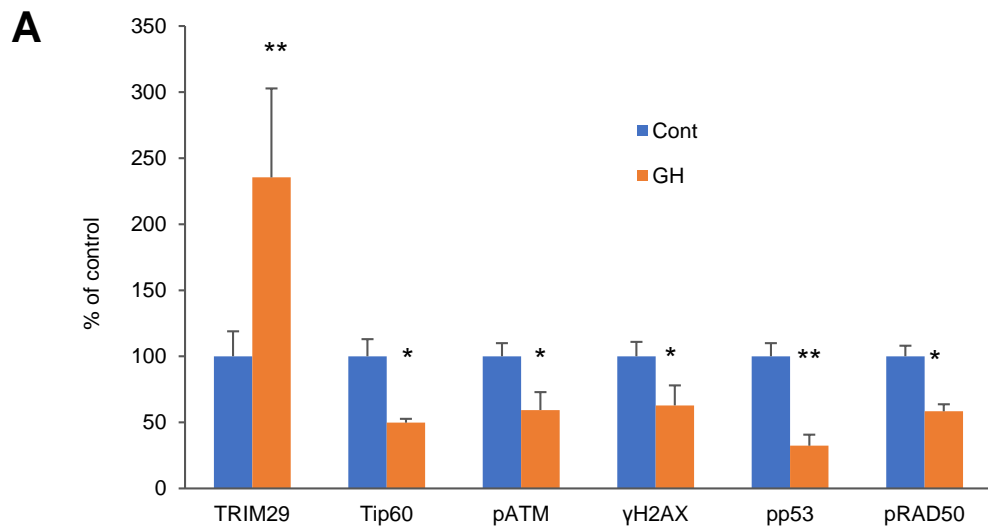


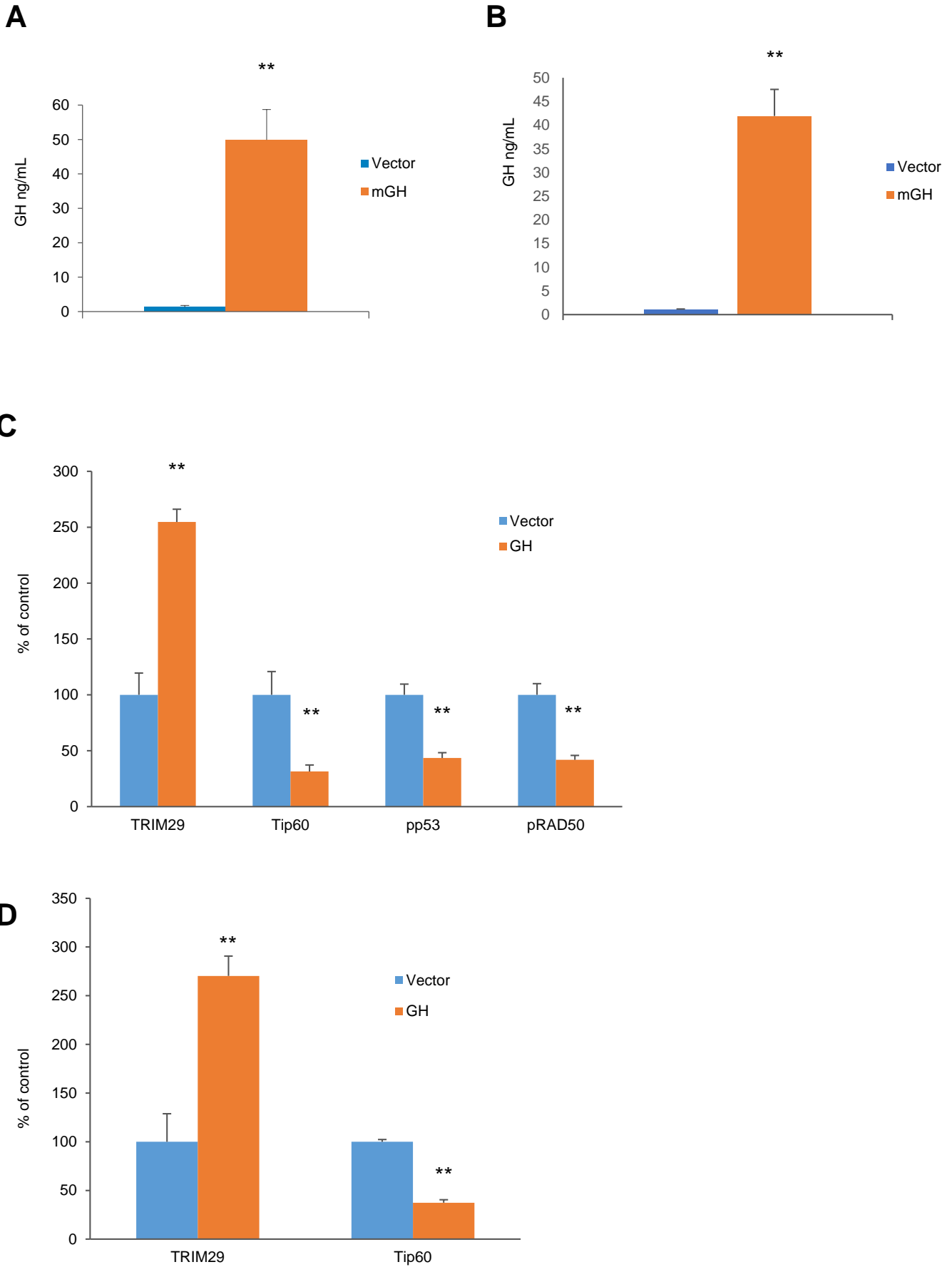
B

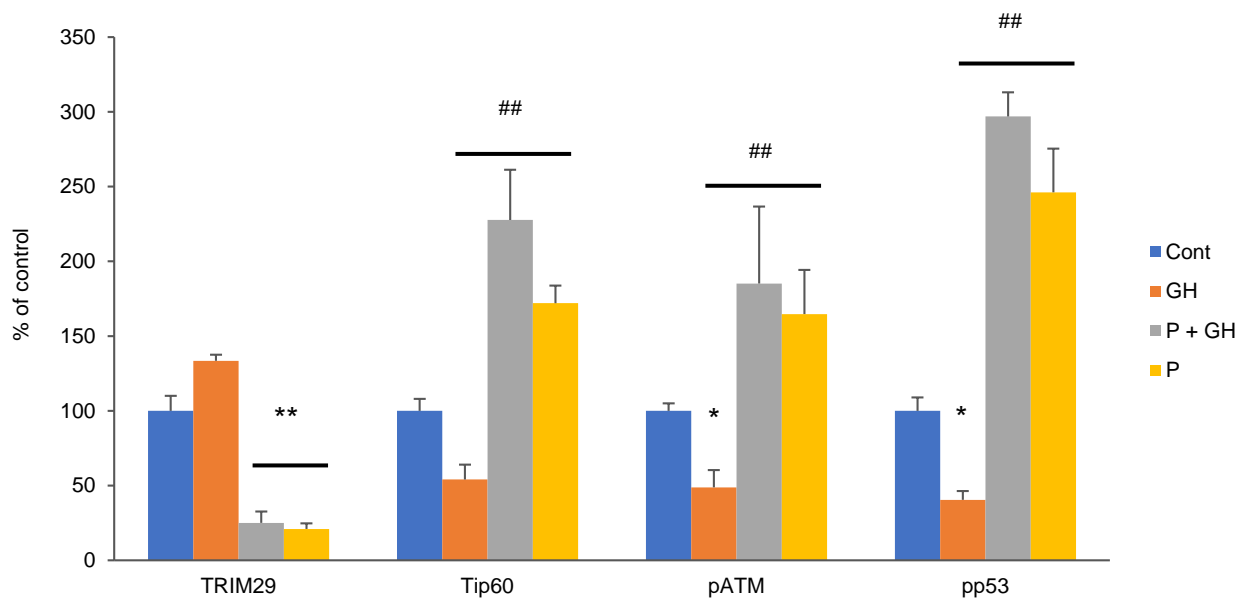
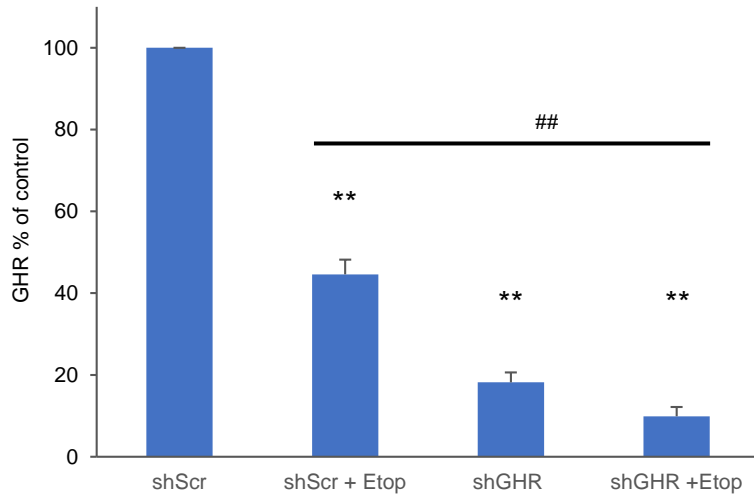


A**B**

A**B**





A**B****C**